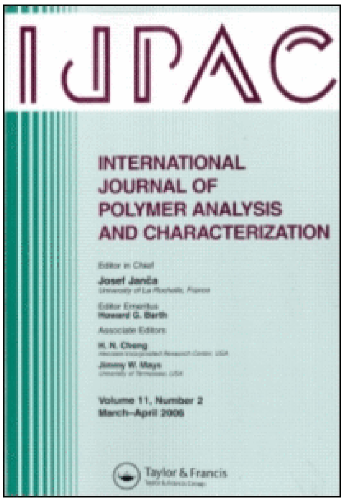

International Journal of Polymer Analysis and Characterization
Publication details, including instructions for authors and subscription information:
http://www.informaworld.com/smpp/title~content=t713646643

Light Scattering and Gel Inhomogeneities

A. Moussaid[a]; H. J. M. Slot[a]; J. G. H. Joosten
[a] Department for Physical, Analytical & Computational Chemistry, DSM Research, Geleen, MD, The Netherlands

To cite this Article Moussaid, A. , Slot, H. J. M. and Joosten, J. G. H.(1995) 'Light Scattering and Gel Inhomogeneities', International Journal of Polymer Analysis and Characterization, 2: 1, 43 — 54

To link to this Article: DOI: 10.1080/10236669508233894

URL: http://dx.doi.org/10.1080/10236669508233894

Int. J. Polymer Analysis & Characterization
1995, Vol. 2, pp. 43–54
Reprints available directly from the publisher
Photocopying permitted by license only

Published in The Netherlands under license by
Gordon and Breach Science Publishers SA
Printed in Malaysia

Light Scattering and Gel Inhomogeneities

A. MOUSSAÏD, H. J. M. SLOT and J. G. H. JOOSTEN*

Department for Physical, Analytical & Computational Chemistry, DSM Research, P.O. Box 18, 6160 MD Geleen, The Netherlands

(Received August 1, 1994; in final form February 7, 1995)

Light Scattering results on polyacrylamide networks show that the scattered intensity changes as different positions of a sample are probed. The scattered intensity from gels, measured by averaging through many different positions, was found to be much larger than the intensity scattered by the equivalent polymer solution. This excess arises from the frozen-in fluctuations due to the presence of cross-links. This additional structure in gels can be enhanced or reduced with conditions of preparation. Modeling a gel by a random network of springs is presented. The resulting scattering properties mimic real gel behavior.

KEY WORDS Light scattering, gels, polyacrylamide, nonergodicity, inhomogeneities, computer simulations

INTRODUCTION

Hydrogels, natural and synthetic, constitute an important class of macroscopic polymer networks. The main microscopic characteristics result from a competition between hydrophobic and hydrophillic interactions. Because of an increasing number of applications [1] and a demand for high performance materials, it is important to describe and understand the molecular architecture of such systems.

Light scattering (LS) and small-angle neutron scattering (SANS) methods are very well suited to provide structural and dynamic information of "particles" dispersed in a medium over both the molecular scale and over larger macromolecular spatial scales.

At length scales probed by LS (>100nm), the scattered intensity by polymer gels turns out to be larger than the scattered intensity by an analogous polymer solution [2–6]. This implies that gels and the equivalent solutions are not the same on a mesoscopic scale. Recently, a nonergodic approach was introduced to interpret light scattering experiments on gels. Nonergodicity, that is, nonequivalence of time-averaged and ensemble-averaged scattered intensities results from limited Brownian motion of polymer segments due to the constraining action of the cross-links [2,7–9]. By regarding a gel as a nonergodic medium, one could conjecture that the scattered intensity is a superposition of two components:

---

*Correspondence to: Dr. Jacques G.H. Joosten, Dept. Physical Chemistry, DSM Research, P.O. Box 18, 6160 MD Geleen, The Netherlands Fax 31-46 767244

Presented at the 7th International Symposium on Polymer Analysis and Characterization, Les Diablerets, Switzerland, May 24–26, 1994.

a fluctuating part, which is *grosso modo* the same for the gel and the corresponding solution, and a frozen-in part due the presence of cross-links. However, the interpretation of measurements is more complex due to the existence in polymer gels, like polyacrylamide (PAM), of a long-range correlation having a spatial scale on the order of several hundreds nm^2, much larger than averaged mesh size [10]. Moreover, recent experiments on polyacrylic acid (PAA) gels, systems similar to PAM, have shown a periodic microstructure and no large-scale inhomogeneities in contrast to the behavior observed in PAM [3,4,11]. In order to control the architecture of gels, the presence of a nontrivial structure at several levels has attracted attention of theorists and experimentalists. In this paper, we present the influence of chemical composition and the gelation processes on the structure of PAM. We also give some additional remarks concerning different experimental findings.

To conclude we present some results concerning modeling a gel by a two-dimensional random network of springs, which appears to mimic the network behavior in a qualitative sense. In particular, some mechanical properties of these model networks were studied [12]. We briefly present an extension of this model, which enables us to calculate the static and dynamic scattering properties with an emphasis on establishing the suggested nonergodic behavior and the presence of a nontrivial structure. Both two- and three-dimensional systems are investigated [13], but only the results concerning the two-dimensional systems are presented here.

SCATTERED LIGHT INTENSITY AND ITS TIME AND ENSEMBLE FLUCTUATIONS

The elementary method of light scattering experiments consists of measuring the scattered intensity $I(\mathbf{q})$ by the sample and its fluctuations in time and space in the direction described by the scattering vector $\mathbf{q}$, which is given by $|\mathbf{q}| = q = (4\pi/\lambda)\sin(\theta/2)$, where λ is the wavelength of the incident beam and θ is the scattering angle. In Figure 1, the influence of sample positions in scattered intensity by a PAM gel and corresponding polymer solution are presented. The samples have been prepared by radical polymerization in aqueous solutions. The procedure of sample preparation and light scattering measurements has been described in previous papers [2,11]. By scanning through various positions in the sample (Fig. 1), a large variation in time-averaged scattered intensity is observed only in the case of a gel. This implies that in this network system we are observing different configurations resulting in different scattered intensities. In a polymer solution, the system can explore sufficient phase space during a single experiment and therefore the time-averaged measurement gives a good estimate of its ensemble-averaged intensities (i.e, $\langle I(q)\rangle_T \equiv \langle I(q)\rangle_E$). By contrast, in a gel, the polymer segments are restricted by the crosslinks to particular regions of the samples and are only able to perform limited Brownian motions about fixed average positions. For a given position and fixed scattering angle, a particular speckle is probed. The time-averaged value of scattered intensity is not, in general, equivalent to an ensemble-averaged measurement (i.e, $\langle I(q)\rangle_T \neq \langle I(q)\rangle_E$).

From the data depicted in Figure 1, one can construct a histogram grouping the time-averaged scattered intensity of various speckles in intervals, resulting in an estimate of the probability distribution function $P(\langle I(q)\rangle_T)$ of the scattered intensity, $\langle I(q)\rangle_T$, sampled over the full ensemble. The probability distribution function shows a cutoff at low inten-

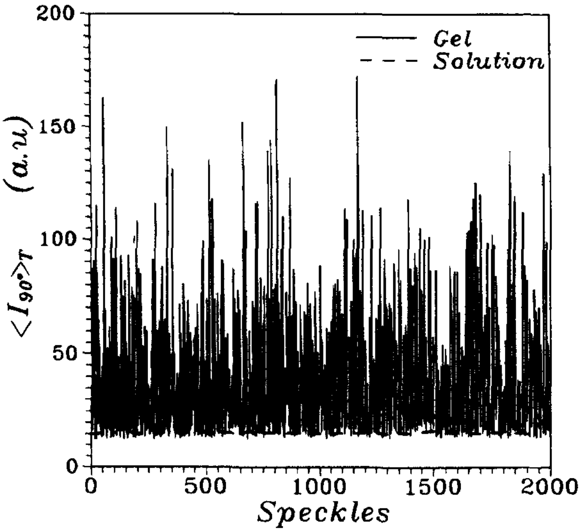

FIGURE 1 Variations of $\langle I(q)\rangle_T$ with a position of sample at scattering angle $\theta = 90°$ for a PAM gel (cross-link monomer ratio $R_c = 1\%$) and equivalent solution (polymer concentration $C_p = 0.1$ g cm^{-3}), prepared at high temperature ($T_p = 70°$C).

sities resulting from the contribution $\langle I_F(q)\rangle_E$ (= $\langle I_F(q)\rangle_T$). In addition to this, one observes an exponential decaying part, characteristic for nonergodic behavior. It is shown that [2,11,14]

$$P(\langle I(q)\rangle_T) \sim H(\langle I(q)\rangle_T - \langle I_F(q)\rangle_T)\exp\left[-\frac{\langle I(q)\rangle_T - \langle I_F(q)\rangle_T}{\langle I(q)\rangle_E - \langle I_F(q)\rangle_T}\right] \tag{1}$$

where $H(x)$ is the Heaviside function, $H(x) = 0$ for $x < 0$ and $H(x) = 1$ for $x > 0$.

More information can be obtained from dynamic light scattering (DLS). Two experimental options are available to determine dynamic structure factor, $f(q, \tau)$, which is by definition an ensemble-averaged quantity.

The first option is the "hard method": the ensemble-averaged intensity correlation functions are constructed by moving the system through a series of many positions (approximately 100 speckles). The dynamic structure factor (or intermediate scattering function) $f(q,\tau)$ is obtained from the representative ensemble-averaged intensity correlation function $g_E^{(2)}(q,\tau)$ as it described in refs. [2] and [11] by using the well-known Siegert relation:

$$g_E^{(2)}(q,\tau) = 1 + \beta^2 |f(q,\tau)|^2 \tag{2}$$

where β is the spatial coherence factor which depends on the number of coherence areas seen by the detector.

The second method is to evaluate $f(q,\tau)$ from a time-averaged intensity correlation function $g_T^{(2)}(q,\tau)$. For that one needs the measurable quantities: $g_T^{(2)}(q,\tau)$ collected at single position (speckle) and its zero-time value $g_T^{(2)}(q,0)$ which can be obtained by extrapolation, the corresponding time-averaged scattered intensity $\langle I(q)\rangle_T$ and the ensemble-averaged scattered intensity $\langle I(q)\rangle_E$. The following equation is then used[2]:

$$f(q,\tau) = 1 + \frac{1}{Y}\left[\sqrt{1 + g_T^{(2)}(q,\tau) - g_T^{(2)}(q,0)} - 1\right] \tag{3}$$

where

$$Y \equiv \frac{\langle I(q)\rangle_E}{\langle I(q)\rangle_T}$$

Figure 2 shows the dynamic structure factor $f(q,\tau)$ obtained from time-averaged intensity correlation functions $g_T^{(2)}(q,\tau)$ for two different speckles and from the ensemble-averaged intensity correlation function $g_E^{(2)}(q,\tau)$. As can be seen from Figure 2, the agreement between the various f(q,τ) values is very good.

One observes that $f(q,\tau)$ decays to a finite value $f(q,\infty)$, characteristic of nonergodic behavior. This asymptotic value is a measure of the frozen-in density fluctuations. By combining static light scattering (SLS) and DLS experiments, one can extract the fluctuating part $\langle I(q)_F\rangle_E$ and a frozen-in part $f(q,\infty)$ from the ensemble-averaged scattered intensity $\langle I(q)\rangle_E$ according to:

$$\langle I(q)_F\rangle_E = \langle I(q)\rangle_E[1 - f(q,\infty)] \tag{4}$$

The fluctuating component arises from the motions of the scatterers around their average positions. It has approximately the same magnitude as the intensity scattered by a solution at the same concentration.

The frozen-in component $f(q,\infty)$ is due to the restriction of the motions of the scatterers. It depends not only on chemical composition but also on the conditions at which the gels are prepared (cf. § II).

Using the first cumulant obtained from the initial slope of $f(q,\tau)$, one can determine the diffusion coefficient $D(q)$ which describes the average decay of all fluctuations: frozen-in and dynamic.

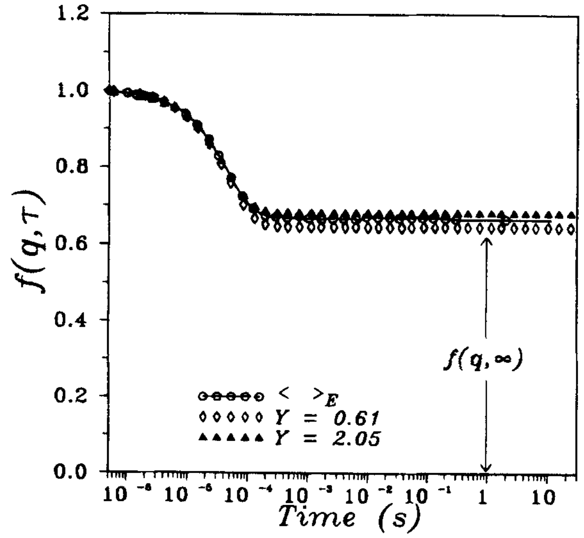

FIGURE 2 Intermediate scattering functions $f(q,\tau)$ for PAM gel (cross-link monomer ratio R_c = 1% and polymer concentration C_p = 0.1 g cm^{-3}) obtained from $g_E^{(2)}(q,\tau)$ and from $g_T^{(2)}(q,\tau)$ at two different speckles, scattering angle $\theta = 90°$, prepared at high temperature (T_p = 70°C).

THE INFLUENCE OF SYNTHESIS ON THE STRUCTURE OF POLYMER NETWORKS

Figure 3 illustrates the effects of synthesis on the ensemble-averaged scattered intensity for PAM system. The first observation is that with decreased preparation temperature (T_p) there is an overall increase in the ensemble-averaged intensity $\langle I(q)\rangle_E$. A second observation is the reduction of scattered intensity in the presence of tetramethylenediamine (TEMED) which is used as an accelerator in gels and solution. Within experimental accu-

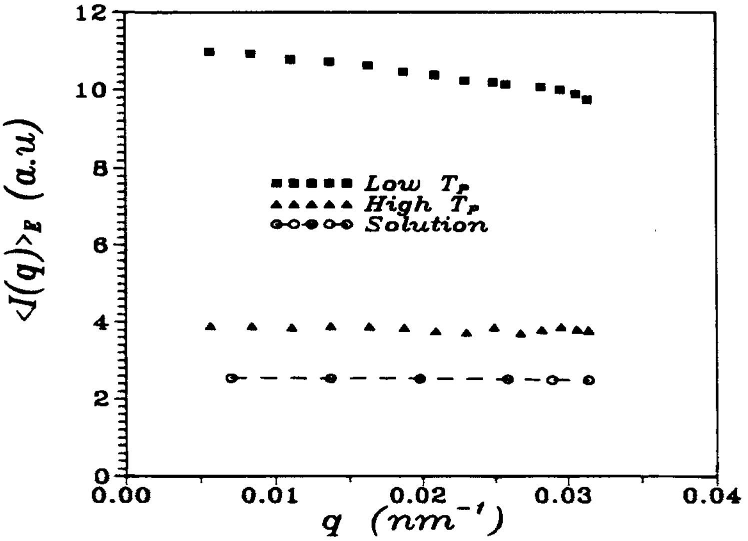

Figure 3a

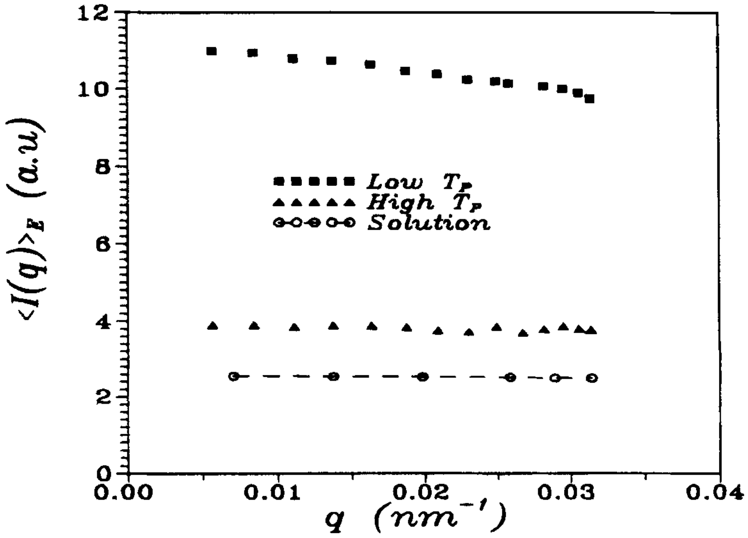

Figure 3b

FIGURE 3 Ensemble-averaged scattering intensity versus scattering vector for the polyacrylamide system with polymer concentration Cp = 3.5% and cross-link monomer ratio Rc = 2% prepared with (Fig. 3a) and without (Fig. 3b) catalyst (TEMED), prepared at high (Tp = 70∞C) and low (Tp = 08∞C) temperatures. The line connecting data points (Fig. 1b) is a guide to the eye.

racy, $\langle I(q)\rangle_E$ is found to be independent of the scattering vector q for the gel prepared at high temperature with TEMED, which reflects the absence of large-scale inhomogeneities.

The same result, that is, no angle dependence of scattered intensity, is found for charged polyacrylic acid PAA and polymethacrylic acid gels (cf. Fig. 4) [3,4,11]. In these systems, the overall electroneutrality requirement prevents a macroscopic phase separation that would force the counterions to follow the polymer chains in the polymer-rich phase [15–17]. For the same reason, large-scale inhomogeneities cannot develop in the course of the gelation process and microdomains are formed at a small scale (≅100 Å) as evidenced by SANS experiments which show a peak in the structure factor (Figure 4).

This implies the existence of polyelectrolyte effect in PAM samples which were prepared with TEMED. Indeed, the charged groups are formed as a result of the hydrolysis of a fraction of amide groups in a basic medium created by TEMED. Infrared experiments show that approximately 0.5% of carboxylate groups COO^- are present in solutions prepared at low and high temperature [18]. At low temperature, hydrolysis takes several days, as was reported by Ilavský et al. [19], in contrast to high temperature where it occurs almost immediately after gelation.

To explain the results reported in Figure 3, one can tentatively propose the following

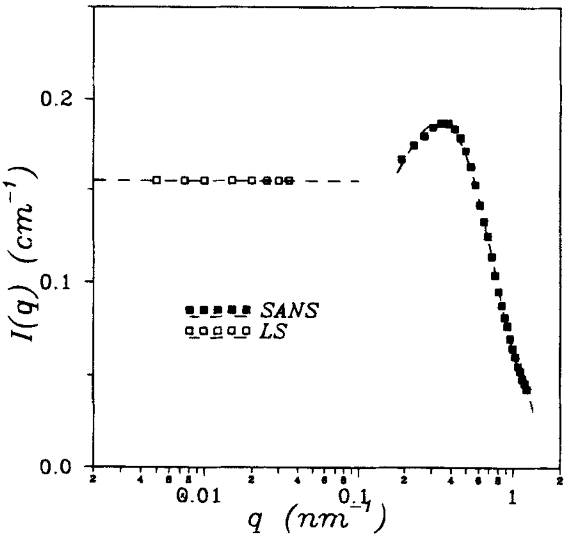

FIGURE 4 Light (LS) and neutron (SANS) scattered intensity *versus* q from PAA gel and corresponding solution at $C_p = 0.05$ g cm^{-3}, $R_c = 0.01$ with ionization degree = 0.5%. The line connecting data points is a guide to the eye.

scheme. In the first stages of the polymerization process, the unreacted cross-linking agent: methylene bisacrylamide, which is hydrophobic, tends to localize in the polymer-dense regions leading to a coagulated structure or aggregates as the gelation reaction proceeds. The size of these aggregates is controlled by the competition between hydrophobic and hydrophillic interactions. The quality of solvent decreases with presence of cross-linking agent and increases with TEMED. At low temperature and high cross-link content, the spatial coagulates are enhanced and critical behavior appears. At high temperature, the solvent quality for bisacrylamide increases as does the speed of hydrolysis. A structural change occurs with formation of microdomains with sizes much smaller than the wavelength of the light.

The above scheme can explain qualitatively the following changes in the scattering curves observed upon changing the gelation temperature as shown in Figure 5. One can observe that the amplitude of the fluctuations of scattered intensity by gels prepared at low T_p is much higher than the amplitude of the fluctuations of scattered intensity by gels prepared at high T_p. Before gelation, more fluctuations with high amplitude are present at reduced temperature, with increasing of the scattered intensity. This increase is essentially due to the frozen-in part as is shown in Figure 6 where the intermediate scattering functions are plotted for the same system prepared at two different temperatures.

To conclude this section, some experimental findings are given. First, if one observes the time-averaged scattered intensity during a long period, a time much longer than the time needed for a realistic light scattering experiment, one notices a slow variation of $\langle I(q) \rangle_T$ (Fig. 7). This result initially appears to be unusual, given the fact that this variation depends on the cross-link content, the size of the sample, and above all on the intensity of the incident beam, could be attributed to, for example, temperature gradients in the sample induced by the laser beam resulting in slow configurational changes. After several hours, the values of time and ensemble-averaged intensities almost coincide in the case of an intense beam. During this time, however, other sources of "noise" can contribute to variations in the scattered intensity. This slow drift with time has been already mentioned [20] but no explana-

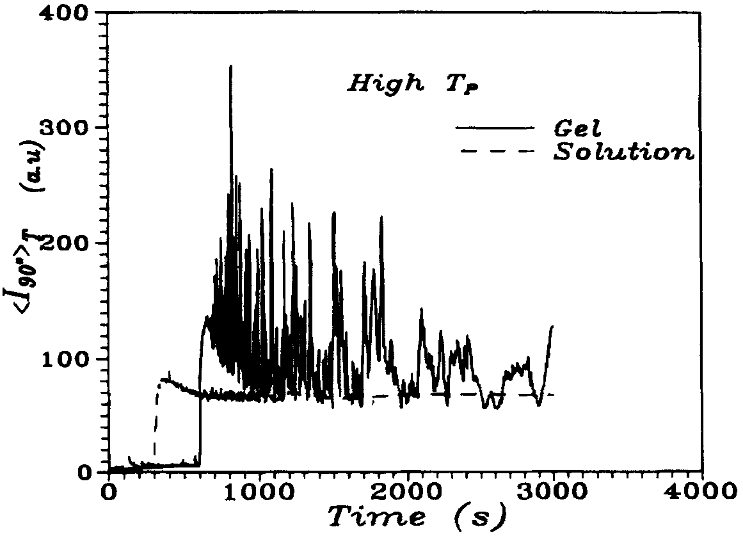

FIGURE 5 Time-averaged scattered intensity at scattering angle $\theta = 90°$ during gelation and polymerization processes at low T_p and high T_p for PAM ($C_p = 0.04$ g cm^{-3} and $R_c = 0.01$).

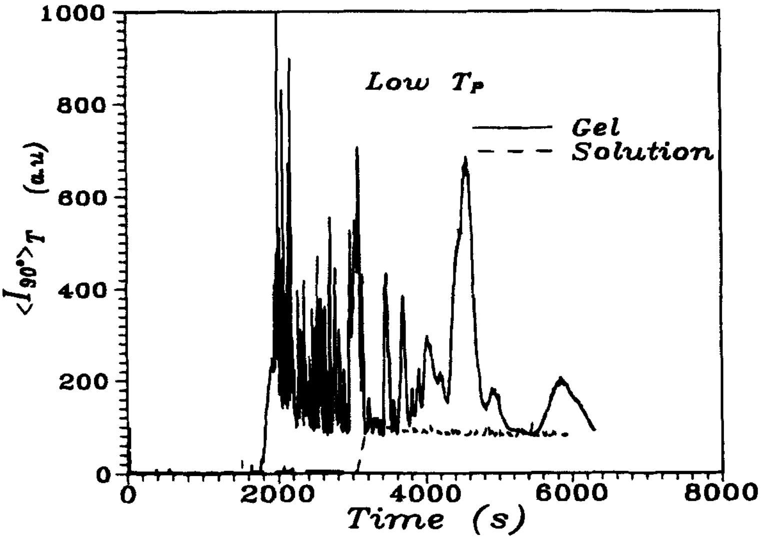

FIGURE 5 (*Continued*)

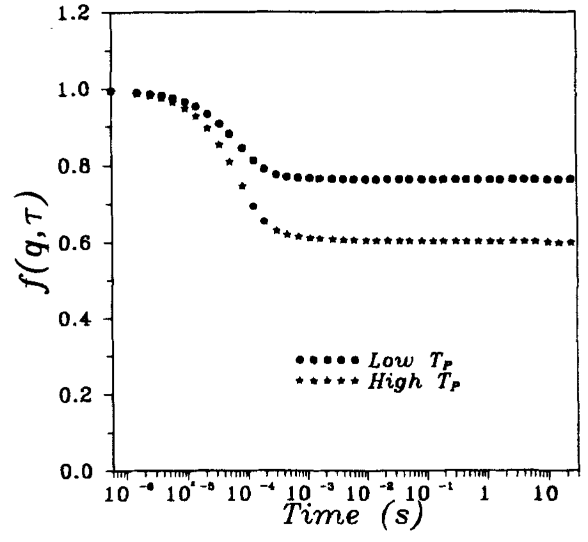

FIGURE 6 Influence of gelation temperature on the PAM gel dynamic structure factor, at scattering angle $\theta = 90°$ ($C_p = 0.04$ g cm^{-3} and $R_c = 0.01$).

tion was given. This slight variation can induce an important change in the shape of the correlation function, even during a short time-averaged measurement. The dilemma between good statistics (where the correlation has to be collected over a long time) and short accurate measurements is obvious. A solution would be to do a series of short time-averaged intensity correlation function (ICF) acquisitions through various position in the sample,

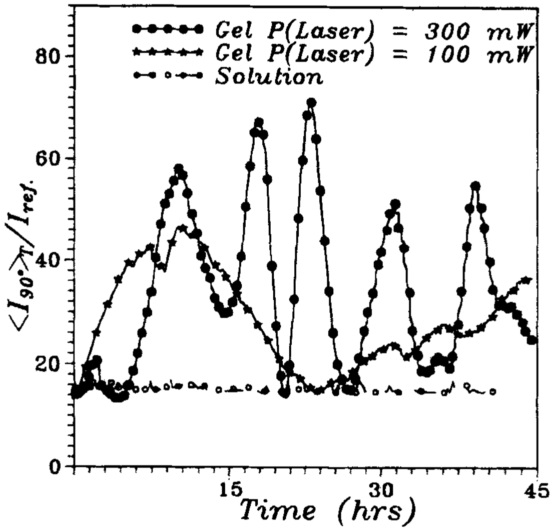

FIGURE 7 Variations of $\langle I(q)\rangle_T$ with time and incidence beam power P(Laser) at scattering angle $\theta = 90°$ for a PAM gel ($R_c = 0.01$) and a solution at $C_p = 0.1$ g cm^{-3}, prepared high temperature ($T_p = 70°C$). The line connecting data points is a guide to the eye.

that is, to perform a "hard method" option to obtain the dynamic structure factor. A more detailed discussion of this phenomenon will be presented in a future publication.

RANDOM NETWORK SIMULATIONS

Contrary to, for instance, the kinetics of gel formation [21] no quantitative theory yet exists that describes the structure and dynamics of a gel. Our aim, therefore, was to study these aspects of a gel qualitatively, using a coarse-grained simulation approach. In this approach, similar as in ref. [12], one particular sample ("scattering volume") or topology of the gel or more precisely the sol/gel system is defined by a two-dimensional graph, initially embedded in a triangular lattice (lattice constant a), whose N^2 vertices are placed within a box of size $V = L^2 = (Na)^2$. Actually, the graph is generated from this triangular lattice via a procedure called "maximum connectivity bond-dilution" (see ref. [12]). The connectivity or coordination of each vertex is at most four and with each edge we associate a harmonic spring with spring-constant K and rest-length $l_0 < a$. Each spring therefore mimics a piece of polymer chain, large enough to exhibit Gaussian behaviour, that is, behave as an entropic spring. In order to prevent the gel from collapsing, periodic boundary conditions consistent with a triangular lattice are employed, leading to an effectively infinite gel. Next to that each vertex or cross-link has a hard-core with radius σ. This "diluted" triangular configuration is then relaxed towards mechanical equilibrium [12]. In Figure 8 representative examples of a diluted unrelaxed and relaxed configuration are shown. It is easy to see the existence of dense and dilute regions in the relaxed state. This result is also shown in Figure 9, where the ensemble-averaged static structure factor $S(q)$

(proportional to the ensemble-averaged scattered intensity) is depicted versus the scattering vector **q** (which is defined here as $q = (2\pi/Na)(n_1 i + n_2 j)$, where **i**, **j** form a basis of a tri-angular lattice and n_1, n_2 are integers ranging in value from $-\infty$ to $+\infty$). It clearly shows the presence of spatial organization.

In order to study the dynamic scattering properties, the degrees-of-freedom of the random network (cross-link—or vertex coordinates) are coupled to a heat bath using a Langevin approach. Thus drag and stochastic (Brownian) forces enter into the equation-

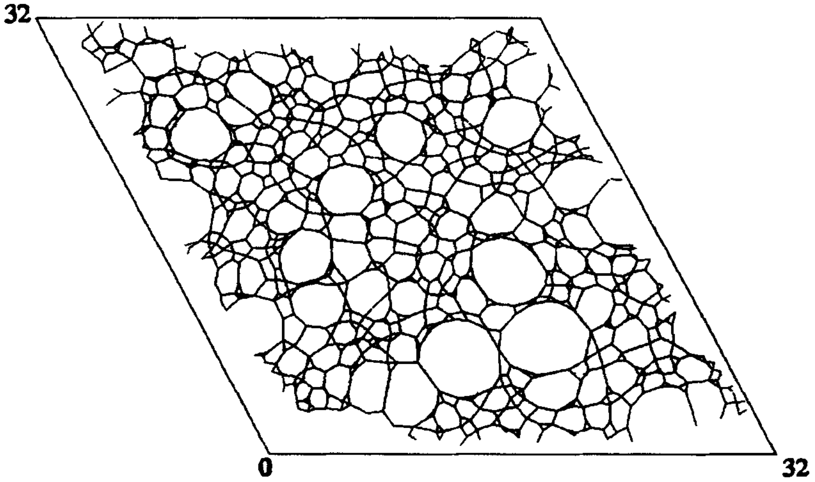

Figure 8a

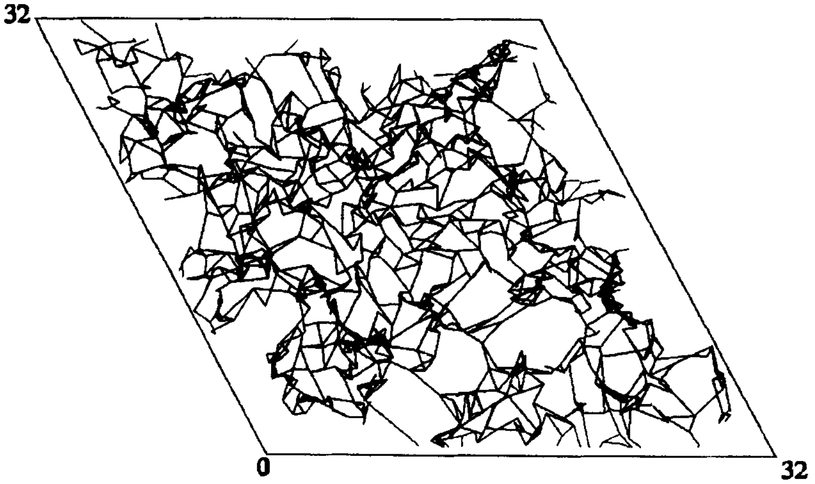

Figure 8b

FIGURE 8 Representations of diluted unrelaxed (Fig. 8a) and relaxed (Fig 8b) two-dimensional hexagonal lattice with maximum connectivity of 4.

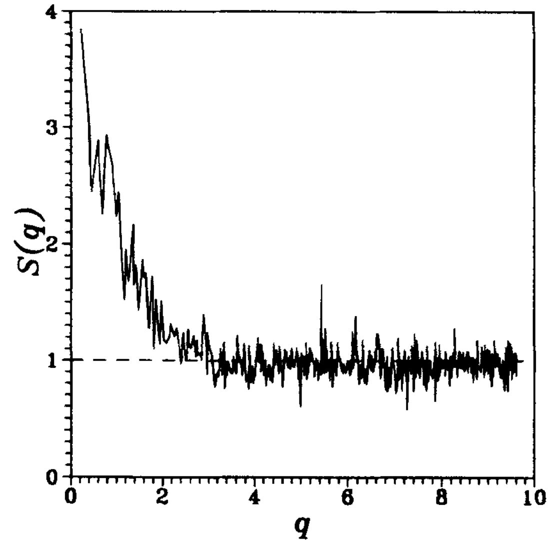

FIGURE 9 Structure factor $S(q)$ of a two-dimensional simulated network with spring-constant $K = 1$ and rest-length $l_0 = 0.1$.

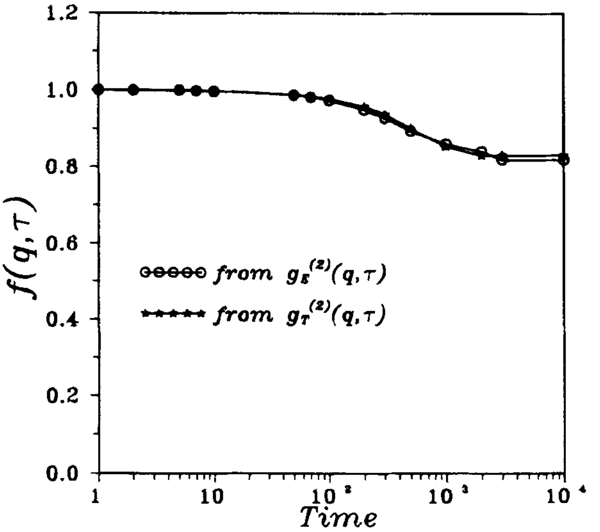

FIGURE 10 Intermediate scattering functions $f(q,\tau)$ for two-dimentional simulated network obtained from $g_E^{(2)}(q,\tau)$ and from $g_T^{(2)}(q,\tau)$ at $|\mathbf{q}| = 0.91$. The line connecting data points is a visual guide.

of-motion for the cross-links. This equation-of-motion in the so-called overdamped limit is then time-integrated to generate configurations of the network having the same topology. By assuming that every cross-link of the network is a scatterer, we can calculate for each of the generated configurations and any given $\mathbf{q}$-vector the total scattered field $E(\mathbf{q},t)$ (all within the first Born approximation). From this quantity we can then calculate the scattered intensity and time-averaged intensity correlation function. Finally, by averaging over different topologies we can calculate the ensemble-averaged scattering properties. The dynamic structure factor $f(q,\tau)$ is obtained from $g_E^{(2)}(q,\tau)$, using Equation (2), and/or from $g_T^{(2)}(q,\tau)$, using Equation (4). The result is plotted in Figure 10. One observes that $f(q,\tau)$ decays to a finite value $f(q,\infty)$, characteristic of nonergodic behavior.

CONCLUSION

Light scattering measurements on gels are complicated by the fact that the scattering intensity changes with time, sample positions and preparation state. The results require special attention. Using a correct procedure to perform and analyze light scattering experiments in gels, one can point out that the gel structure depends on the gelation process. In a polymer gel, the presence of additional structures or "inhomogeneities" is due to crosslinks and the amplitude of such structures can be controlled by the gelation temperature. Theoretically the effect of heterogeneities on networks have been discussed[22-24] but there is no a full microscopic description taking frozen-in fluctuations into account. A computer simulation mimics experimental results and seems to generate structures with inhomogeneities.

References

1. *Encyclopedia of Polymer Science and Engineering*, 2nd ed.; H. F. Mark, N. M. Bikales, C. G. Overberger, and G. Menges, Eds.; Wiley Interscience: New York, 1985; Vol. 7, pp 783–807.
2. J. G. H Joosten, J. L. McCarthy, and P. N. Pusey, *Macromolecules*, **24**, 6690 (1991).
3. A. Moussaïd, J. P. Munch, F. Schosseler, and S. J. Candau, *J. Phys. II (Fr.)*, **1**, 637 (1991).
4. S. J. Candau, A. Moussaïd, and J. G. H. Joosten, *Makromol. Chem., Macromol. Symp.*, **72**, 175 (1993).
5. S. J. Candau, J. Bastide, and M. Delsanti, *Adv. Polym. Sci.*, **44**, 27 (1982).
6. E. Mendes, B. Girard, C. Picot, M. Buzier, F. Boué, and J. Bastide, *Macromolecules*, **26**, 6873 (1993).
7. P. N. Pusey and W. van Megen, *Phys. Rev. Lett.*, **59**, 2083 (1987).
8. J. G. H Joosten, E. T. F Geladé, and P. N Pusey, *Phys. Rev. A*, **42**, 2161 (1990).
9. J. G. H Joosten, *Progr. Colloid Polym. Sci.*, **91**, 149 (1993).
10. P. G. de Gennes, *Scaling Concepts in Polymer Physics*; Cornell University: Ithaca, New York, 1979.
11. A. Moussaïd, S. J. Candau and J. G. H Joosten, *Macromolecules*, **27**, 2102 (1994).
12. M. J. Grimson, *Mol. Phys.*, **74**, 1097 (1991).
13. H. Slot, A. Moussaïd and J. G. H Joosten, to be published.
14. B. Saleh, *Photoelectron Statistics*; Springer-Verlag: Berlin, 1978; Springer Series in Optical Sciences, Vol. 6, pp 114–156; E. Jakeman, In *Photon Correlation and Light Beating Spectroscopy*; H. Z. Cummins and E. R. Pike, Eds.; Plenum Press: New York, 1974, pp 75–149.
15. V. Borue and I. Erukhimovich, *Macromolecules*, **21**, 3240 (1988).
16. J. F. Joanny and L. Leibler, *J. Phys. (Fr.)*, **51**, 545 (1990).
17. A. Moussaïd, F. Schosseler, J. P. Munch, and S. J. Candau, *J. Phys. II (Fr.)*, **3**, 573 (1993).
18. A. Moussaïd and J. G. H. Joosten, unpublished results.
19. M. Ilavský, J. Hrouz, J. Stejskal, and K. Bouchal, *Macromolecules*, **17**, 2868 (1984).
20. R. Skouri, J. P. Munch, F. Schosseler, and S. J. Candau, *Europhys. Lett.*, **23**, 635 (1993).
21. *Kinetics of Aggregation and Gelation*; F. Family and D. P. Landau, Eds.; North-Holland: Amsterdam, 1984.
22. K. Dušek and W. Prins, *Adv. Polym. Sci.*, **6**, 1, (1969).
23. J. Bastide, L. Leibler and J. Prost, *Macromolecules*, **23**, 1821 (1990).
24. T. A. Vilgis and G. Heinrich, *Phys. Rev. E*, **49**, 2167 (1994).